Emergence of quasiequilibrium state and energy distribution for the beads-spring molecule interacting with a solvent

Tatsuo Yanagita [*]
Department of Engineering Science, Osaka Electro-Communication University, Neyagawa 572-8530, Japan

Tetsuro Konishi [†]
General Education Division, College of Engineering, Chubu University, Kasugai 487-8501, Japan

(Received 1 February 2021; accepted 2 August 2021; published 10 September 2021)

We study the energy distribution during the emergence of a quasiequilibrium (QE) state in the course of relaxation to equipartition in slow-fast Hamiltonian systems. A bead-spring model where beads (masses) are connected by springs is considered. The QE lasts for a long time because the energy exchange between the high-frequency vibrational and other motions is prevented when springs in the molecule become stiff. We numerically calculated the time-averaged kinetic energy and found that the kinetic energy of the solvent particles was always higher than that of the bead in a molecule. This is explained by adopting the equipartition theorem in QE, and it agrees well with the numerical results. The energy difference can help determine how far the system is from achieving equilibrium, and it can be used as an indicator of the number of frozen or inactive degrees existing in the molecule.

DOI: 10.1103/PhysRevE.104.034209

I. INTRODUCTION

Relaxation to equipartition in Hamiltonian dynamical systems is a long-standing problem that has been extensively studied; for example, in the coupled oscillatory chain, i.e., the Fermi-Pasta-Ulam systems [1]. Systems considered in these studies are nearly integrable, and the relaxation to equipartition is often prevented by the KAM tori. Thus, there is an energy threshold to determine whether an equipartition state is established [2]; further, the relaxation exhibits multiple stages and nonmonotonic behavior [3]. The energy transfer between fast and slow subsystems becomes very slow when the difference between timescales in the subsystems is very large. This effect was first noticed by Boltzmann and Jeans [4]; subsequently, Landau and Teller presented the exponential law of relaxation time [5–7]. This effect has been confirmed numerically for a classical gas of diatomic molecules [8]; further, such systems are known to prevent equipartition [9–11]. In addition, a relaxation process is considered in the Hamiltonian dynamics of self-gravitating systems [12–14]. These systems demonstrate the existence of quasiequilibrium and slow relaxation to the equilibrium. Further, in the context of the function of proteins, the energy transfer occurring out-of-equilibrium plays a key role, and there exists a bottleneck for this energy transfer [15].

We consider the dynamics of the bead-spring model—masses connected by springs—that can be adopted for modeling of protein and DNA. Such models have practical importance and play significant roles in various fields [16]. In terms of the function of these materials, it is important to consider the dynamic activity during relaxation to equilibrium.

In our previous studies, we focused on the relaxation process in a serially connected bead-spring molecule. When the molecule is surrounded by a solvent, the beads exchange energy through collisions with solvent particles, and the system relaxes to equipartition, where all kinetic energies of the beads in the molecule and solvent particles become equal. We regard the kinetic energy of each component as an indicator of dynamical activeness. Further, we reported that the distribution of the time-averaged energy of each bead is not uniform over a long time, which we call the quasiequilibrium (QE) [17,18]. If the spring constant k of the spring between the beads in the molecule is large, then the duration of QE obeys $\exp(c\sqrt{k})$, which is a typical feature of the Boltzmann-Jeans type relaxation [18].

In this study, we consider the kinetic energy per bead in the molecule and the solvent particle in the QE. We consider two types of molecules: chain and network. These are respectively sparsely and densely connected. We numerically showed that the time-averaged kinetic energy of the solvent particles was larger than that of the beads in the bead-spring molecule in QE. The difference between the time-averaged kinetic energy of the molecule and the solvent depends on the type of molecule (the connection topology), the size of the molecule, and the number of solvent particles. We theoretically clarify the difference in the kinetic energies by adopting the equipartition theorem. The key point of the emergence of the energy difference in QE is the existence of "frozen" degrees, which comes from high-frequency vibrations in the molecule. These vibrational motions are frozen in the sense that the energy exchange to the other part is prevented. We estimate the number of frozen degrees and adopt the equipartition theorem to the QE state, and we analytically determine the extent to which

[*] yanagita@osakac.ac.jp
[†] tkonishi@isc.chubu.ac.jp

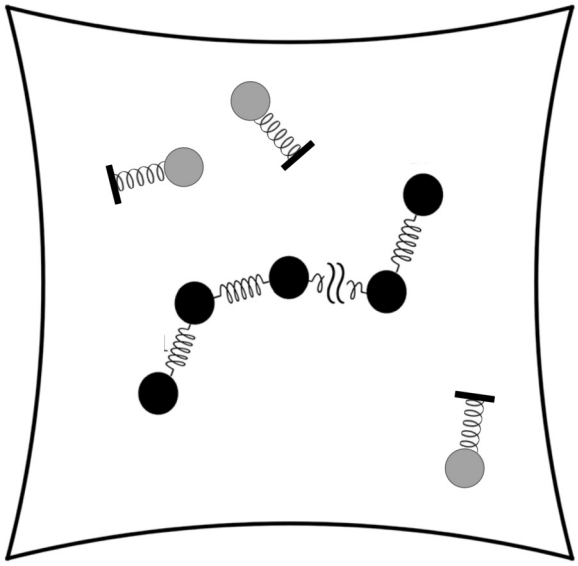

FIG. 1. Schematic of the bead-spring chain molecule in solvent particles. The beads are serially connected by linear springs. The figure shows the chain molecule with $N_b = N$ and the number of solvent particles $N_s = 3$.

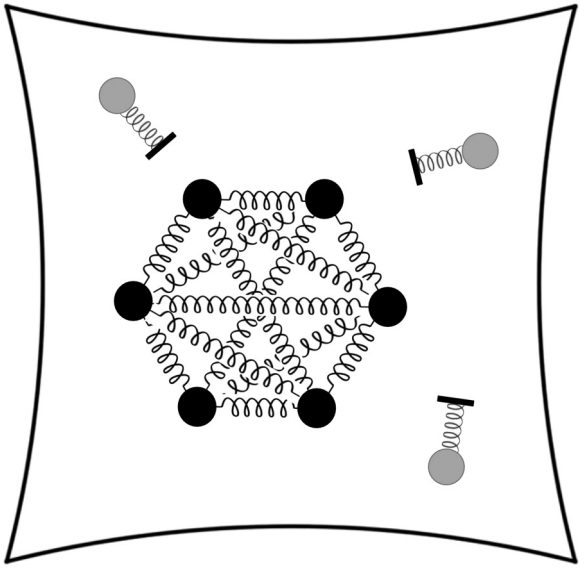

FIG. 2. Schematic of the bead-spring network molecule. The beads are densely connected with linear springs. The connection topology considered here is a complete graph. The figure shows the network molecule with $N_b = 6$ and the number of solvent particles $N_s = 3$.

the kinetic energy of the solvent particle is higher than that of the molecule. The theoretical analysis is in good agreement with the numerical results.

The remainder of this manuscript is organized as follows: In Sec. II, we introduce a system of bead-spring molecules in a solvent and present the Hamiltonian of the models. The numerical method and parameter settings are discussed in Sec. III. The numerical results are shown in Sec. IV. In Sec. IV A, the slow relaxation to equipartition and the emergence of QE are shown where the kinetic energy of the solvent particles is higher than that of beads in a molecule. We show the kinetic energy difference between beads in a molecule and solvent particles in Sec. IV B. Numerical results for network molecules, which are beads connected by springs to form a network topology that models a densely connected molecule, are presented in Sec. IV C. The theoretical explanation for the numerical results is provided based on the equipartition theorem in Sec. V. Finally, Sec. VI summarizes this work and provides a brief outlook.

II. BEAD-SPRING MOLECULE IN SOLVENT

This study considers a model system known as the bead-spring model [16], in which masses are connected by springs and interactions occur with other surrounding particles. Hereafter, we refer to the bead-spring part as a molecule and the other particles as solvent particles. The connective structure of the bead-spring part can be a serial or complex network. These bead-spring molecules are in the external potential, and they interact with the solvent particles. For simplicity, we consider that the beads are connected by linear springs. Even with the linear springs used in this study, the system is nonlinear and exhibits strong chaotic behavior. The schematics of the models for the serial and network connections are shown in Figs. 1 and 2, respectively.

The Hamiltonian of the system is given by

$$H = H_{\mathrm{mol}} + H_{\mathrm{sol}} + H_{\mathrm{int}}, \tag{1}$$

$$H_{\mathrm{mol}} = \sum_{i=1}^{N_b} \frac{p_i^2}{2m} + \sum_{i\neq j}^{N_b} \frac{k_{i,j}}{2}(|\overrightarrow{r_j} - \overrightarrow{r_i}| - \ell_{i,j})^2 + \sum_{i=1}^{N_b} U_{\mathrm{ext}}(\overrightarrow{r_i}), \tag{2}$$

$$H_{\mathrm{sol}} = \sum_{\alpha=1}^{N_s} \frac{p_\alpha^2}{2m} + \sum_{\alpha=1}^{N_s} U_{\mathrm{ext}}(\overrightarrow{r_\alpha}), \tag{3}$$

$$H_{\mathrm{int}} = \sum_{i,\alpha;\mathrm{pair}} U_{\mathrm{int}}(|\overrightarrow{r_i} - \overrightarrow{r_\alpha}|) + \sum_{\alpha,\beta;\mathrm{pair}} U_{\mathrm{int}}(|\overrightarrow{r_\alpha} - \overrightarrow{r_\beta}|), \tag{4}$$

where N_b and N_s denote the number of beads in the molecule and solvent particles, respectively; subscripts i and j represent the indices of beads in the molecule, and α and β represent the indices of solvent particles. Here $\overrightarrow{r_i}$ and $\overrightarrow{r_\alpha}$ represent the positions of beads i and solvent particles α, respectively, where bead i belongs to the molecule and particle α belongs to the solvent, while $\overrightarrow{p_i}$ and $\overrightarrow{p_\alpha}$ are the momenta conjugate to $\overrightarrow{r_i}$ and $\overrightarrow{r_\alpha}$, respectively. The natural length of the spring between i and j beads is $\ell_{i,j}$. Solvent particles interact with beads in the molecule via the potential U_{int}

$$U_{\mathrm{int}}(r) = \begin{cases} \frac{k_\alpha}{2}(r - l_\alpha)^2 & \cdots r < l_\alpha, \\ 0 & \cdots r \geqslant l_\alpha. \end{cases} \tag{5}$$

The external potential U_{ext}, as shown in Fig. 1, confines the molecule and solvent in a finite region via

$$U_{\mathrm{ext}}(\overrightarrow{r}) = a \sum_{n=1}^{N_{\mathrm{wall}}} ||\overrightarrow{r} - \overrightarrow{R}_n| - L_{\mathrm{wall}}|^{-6}. \tag{6}$$

It breaks the rotational symmetry and thus prevents the conservation of the angular momentum. Here we use the following parameters: $a = 100/N_{\rm wall}$, $N_{\rm wall} = 4$, $\vec{R}_j \equiv (R, 0)$, $(0, R)$, $(-R, 0)$, $(0, -R)$, and $R \equiv L_{\rm wall} + \sqrt{R_{\rm wall}^2 - L_{\rm wall}^2}$. $R_{\rm wall}$ and $L_{\rm wall}$ define the curvature of the wall and the size of the finite region, respectively. This potential resembles that used in dispersing billiards [19], where systems do not have any conserved quantities other than the total energy, and the orbit obtained from a long time simulation can be well approximated by the microcanonical distribution.

We consider two types of bead-spring molecules in two-dimensional space: bead-spring chain and bead-spring network molecules. These models respectively correspond to the two cases in which beads in the molecule are sparsely and densely connected by springs.

A. Bead-spring chain molecule

The primary characteristic of a chain-type molecule is that beads are connected serially with springs (Fig. 1). The following homogeneous parameters are used here:

$$k_{i,j} = \begin{cases} k & (i = 1, \ldots, N_b - 1,\ j = i + 1), \\ 0 & \text{otherwise} \end{cases} \tag{7}$$

and $\ell_{i,j} = 1$ $(i = 1, \ldots, N_b - 1,\ j = i + 1)$.

For the initial condition of the chain molecule, all springs between beads were set to be the natural length, and the initial positions of beads $\overrightarrow{r_i}(0) = (x_i(0), y_i(0))$ are

$$x_i(0) = i - (N + 1)/2,\ y_i(0) = 0\ \ (i = 1, \ldots, N_b), \tag{8}$$

respectively, which is the center of the mass that is set to be the origin $\vec{r}_{\rm c.m.}(0) = \sum_i m_i \vec{r}_i(0) / \sum_i m_i = (0, 0)$. In addition, the initial velocity of the chain molecule sets

$$\begin{aligned} \dot{x}_i(0) &= v_0 \cos(\theta_0), \\ \dot{y}_i(0) &= v_0 \sin(\theta_0)\ \ (i = 1, \ldots, N_b), \end{aligned} \tag{9}$$

where the initial direction of the motion θ_0 is a random number selected from a uniform distribution in the interval $[0, 2\pi]$. Thus, the total energy of the chain molecule is $K_{\rm chain} = \frac{M}{2} v_0^2 \equiv E_0$, where $M = mN_b$ is the total mass. For external potential, we use $L_{\rm wall} = N_b$ and $R_{\rm wall} = 4L_{\rm wall}$.

B. Bead-spring network molecule

As shown below, the number of springs is a crucial parameter that determines the energy distribution during QE. Thus, it is interesting to consider the bead-spring network molecule where the connections of beads in the molecule are represented by the adjacency matrix $k_{i,j}$. To contrast the chain molecule, we consider the complete graph as the connection topology of the beads in the molecule where all pairs of beads in the molecule are connected by springs. The Hamiltonian of the network molecule is

$$H = H_{\rm net} + H_{\rm sol} + H_{\rm int}, \tag{10}$$

$$H_{\rm net} = \sum_{i=1}^{N_b} \frac{p_i^2}{2m} + \sum_{i=1}^{N_b - 1} \sum_{j=i+1}^{N_b} \frac{k_{i,j}}{2} (|\overrightarrow{r_j} - \overrightarrow{r_i}| - \ell_{i,j})^2. \tag{11}$$

The Hamiltonians of solvent $H_{\rm sol}$ and the interaction parts $H_{\rm int}$ are the same as in Eqs. (3) and (4). The external potential $U_{\rm ext}$ is the same as in Eq. (6). A schematic of the network molecules is shown in Fig. 2.

For the initial condition, we consider that each bead in the molecule is located at the vertex of the N_b equilateral polygon placed on the unit circle. In particular, the initial positions of the beads $\overrightarrow{r_i}(0) = (x_i(0), y_i(0))$ are

$$\begin{aligned} x_i(0) &= \cos(2\pi i/N_b), \\ y_i(0) &= \sin(2\pi i/N_b)\ \ (i = 1, \ldots, N_b), \end{aligned} \tag{12}$$

respectively. We set the natural lengths of springs to $\ell_{i,j}^2 = [x_i(0) - x_j(0)]^2 + [y_i(0) - y_j(0)]^2$. The natural lengths of springs in the network molecule have different values and are set according to the initial distances between beads; thus, the potential part of the Hamiltonian Eq. (2) is zero. For external potential, we use $L_{\rm wall} = 4.5$ and $R_{\rm wall} = 4L_{\rm wall}$.

III. NUMERICAL METHOD AND PARAMETER SETTINGS

For time integration, we use the fourth-order implicit Runge-Kutta method with a time interval $\delta t = 0.001/\sqrt{k}$. The method is known to be symplectic [20], and the total energy is well conserved in our numerical simulations.

Throughout the paper, all masses are the same, i.e.,

$$m_\alpha = m_i = m = 1 \text{ for all } i \text{ and } \alpha. \tag{13}$$

Further, we set that all spring coefficients between beads in the molecule to the same value:

$$k_{i,j} = k \text{ for } i, j = 1, \ldots, N_b. \tag{14}$$

The initial distances between the positions of the solvent particles, which were randomly set according to the distances between the pairs of particles, were larger than $l_\alpha = 1$; $|\overrightarrow{r_\alpha} - \overrightarrow{r_\beta}| > \ell_\alpha$ and $|\overrightarrow{r_i} - \overrightarrow{r_\alpha}| > \ell_\alpha$ for all α and β, and i and α, respectively. Therefore, the interaction energy between the beads and solvent particles is initially zero, i.e., $H_{\rm int} = 0$. For solvent particles, the kinetic energy was set to be zero $p_\alpha = 0$ for all α. All momenta of the beads in the molecule are set to the same value, which means that the molecule has only the kinetic energy of the center of gravity. We can say that the above initial condition is a scenario in which a "hot" molecule is set in a "cold" solvent. In other words, the system is highly inhomogeneous in the sense that all energy is placed into the kinetic part of the beads in the molecule, and the other parts of the energy are set to zero.

Although beads are connected with linear springs, the system is nonlinear and behaves chaotically both with and without external potential. A periodogram of the time series of the positions of a terminal bead is shown in Fig. 3.

The characteristic timescale $t_{\rm coll}$ of collisions between a bead in the molecule and the external boundary is $t_{\rm coll} \sim 7.4$ when $E_0 = 0.1$ and $k = 10$. A collision between the bead in the molecule and the boundary is detected when the $U_{\rm ext}(\vec{r}_i)$ exceeds a threshold value $\tilde{U}_{\rm ext} = 10^{-4}$. The characteristic timescale is estimated by averaging the time interval between collision events in $t \in [0, 10^4]$.

As we are interested in the energy distribution during the QE state, we focus on the scenario wherein a fast timescale

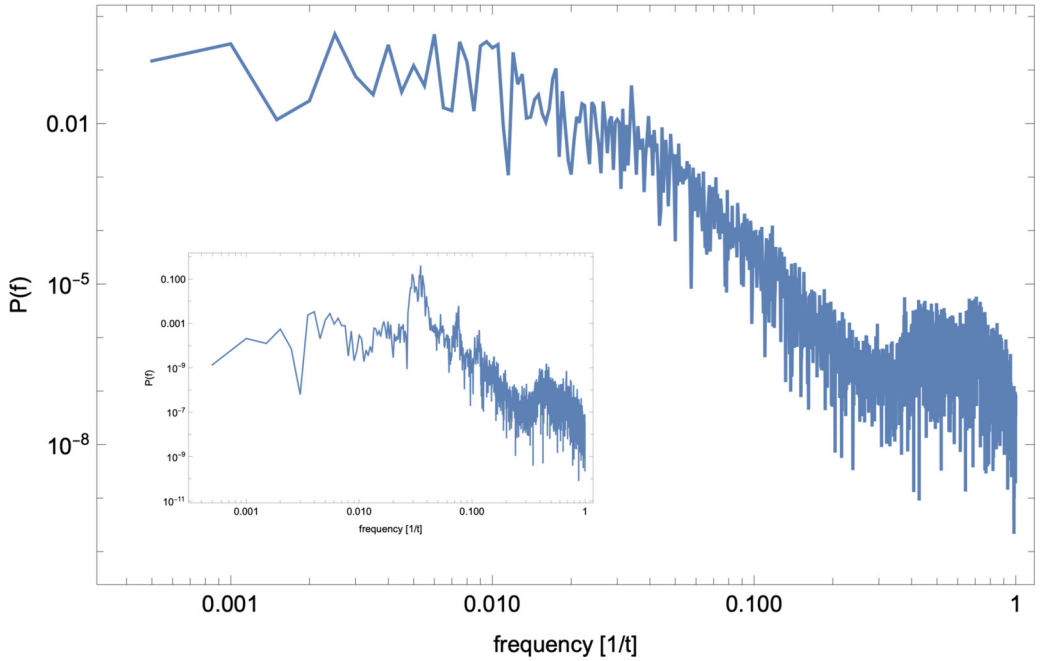

FIG. 3. The periodogram of the time series of x coordinate of the terminal bead $x_1(t)$ for $t \in [0, 2000]$ is shown. The parameters are $k = 10$, $N_b = 4$, $N_s = 2$, $\ell_{i,j} = \ell_\alpha = 1$, $m = 1$, $k_\alpha = 1$, and $E_0 = 0.2$. The inset is the periodogram of the time series of the $x_1(t) - x_{\text{c.m.}}(t)$ for the bead-spring without solvent and the external potential, where $x_{\text{c.m.}}(t)$ is the x coordinate of the center of the mass for the bead-spring molecule.

results from the high-vibrational motion of the molecule, which comes from a large spring constant; thus, we set $k = 1000$. For the interaction between the molecule and solvent, we set $k_\alpha = 1$ in Eq. (5).

IV. NUMERICAL RESULTS

To observe the relaxation process, we measured the time-averaged kinetic energy $K_i(t)$ of the beads and solvent particles, and the spring energies $V_{i,j}(t)$ in the molecule, which are defined as

$$K_i(t) \equiv \frac{1}{t}\int_0^t \frac{p_i^2(t')}{2m}\,dt', \tag{15}$$

$$V_{i,j}(t) \equiv \frac{1}{t}\int_0^t \frac{k_{i,j}}{2}(|\overrightarrow{r_j}(t') - \overrightarrow{r_i}(t')| - \ell_{i,j})^2\,dt'. \tag{16}$$

We averaged the time-averaged kinetic energy over all beads and the particles as

$$\overline{K_{\text{mol}}}(t) = \frac{1}{N_b}\sum_{i=1}^{N_b} K_i(t), \tag{17}$$

$$\overline{K_{\text{sol}}}(t) = \frac{1}{N_s}\sum_{\alpha=1}^{N_s} K_\alpha(t), \tag{18}$$

$$\overline{V_{\text{mol}}}(t) = \frac{1}{N_k}\sum_{i\neq j}^{N_b} V_{i,j}(t), \tag{19}$$

where $N_k = \sum_{i\neq j}\Theta(k_{i,j})$ is the number of springs in the molecule, and $\Theta(x)$ is the Heaviside function. Because the time evolution of the above kinetic energies depends on the initial condition, the initial moment of the molecule, and the initial position of the solvent particles, we further averaged it over $\mathscr{M}$ samples starting from different initial conditions. The initial positions of the beads in the molecule are given by Eqs. (8) and (12) for chain and net molecules respectively; we randomly change the initial direction of momenta randomly by selecting from a uniform distribution in interval $[0, 2\pi]$.

A. Slow relaxation to equipartition and the emergence of quasiequilibrium

We demonstrate the relaxation to equipartition through the short-chain molecule with the number of beads $N_b = 3$ surrounded by two solvent particles $N_s = 2$. The evolution of the time-averaged kinetic energies of the chain molecule and solvent and the potential energy of the spring are shown in Fig. 4. When the two spring constants are equal, $k = k_\alpha = 1$, there are no fast or slow-timescales in the system. The kinetic energy initially assigned to the chain molecule is distributed gradually into other parts such as the vibrational and interaction parts. As shown in Fig. 4(a), the system relaxes to the equipartition wherein all kinetic energies for the beads and solvent particles are equal. The solid curve shows the kinetic energy of the chain molecule $\overline{K_{\text{mol}}}(t)$, and it almost monotonically decreases and converges to a stationary value. As shown in the dashed curve, the kinetic energy of solvent $\overline{K_{\text{sol}}}(t)$ monotonically increases from zero and converges to the same stationary value as that of the chain molecule. The spring energy $\overline{V_{\text{mol}}}(t)$ shown by the dotted line gradually increases from zero and converges to a stationary value, that is, half of the stationary value of the time-averaged kinetic energy because we consider two-dimensional space,

$$\lim_{t\to\infty}\overline{V_{\text{mol}}}(t) = \lim_{t\to\infty}\frac{\overline{K_{\text{mol}}}(t)}{2}.$$

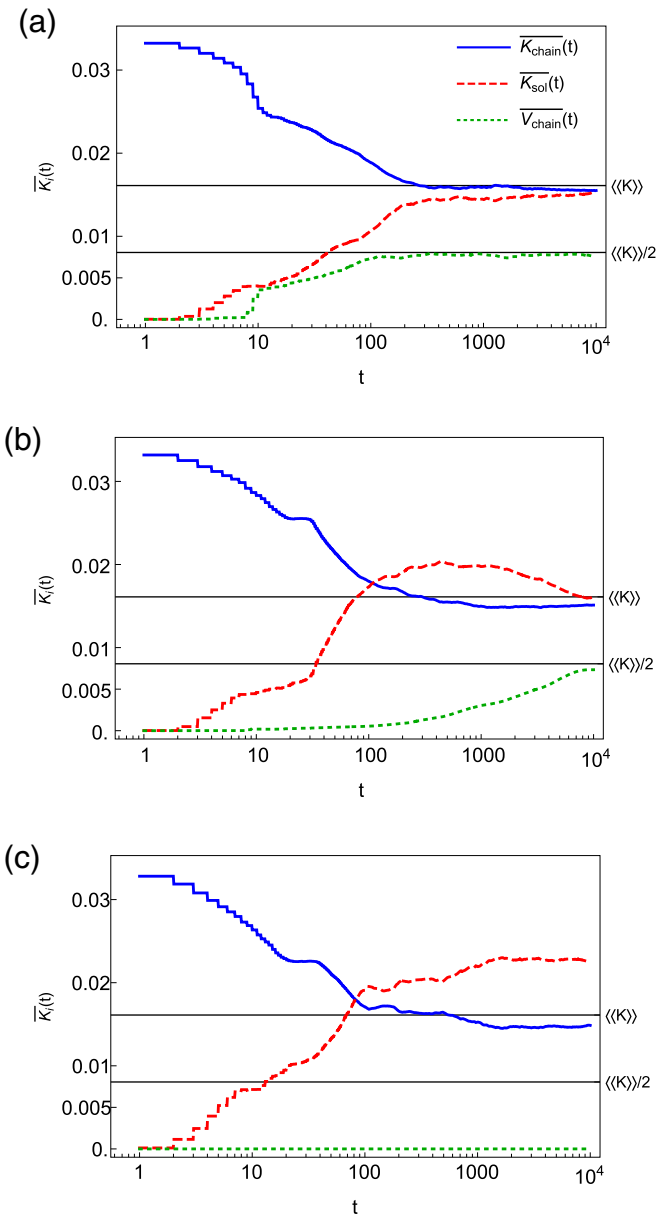

FIG. 4. Relaxation process to equipartition. Kinetic energy of chain molecules and solvent particles as a function of the averaging time. The solid, dashed, and dotted curves represent the kinetic energies of the chain molecule and solvent particles, and the potential energy of the springs, respectively. The horizontal solid lines represent the estimated energy level when the equipartition is established. The spring constants between chain beads are (a) $k = 1$, (b) $k = 10$, and (c) $k = 1000$. The sample average is taken over 20 different initial conditions. $N_b = 3, N_s = 2, \ell_{i,j} = \ell_\alpha = 1, m = 1, k_\alpha = 1$, and $E_0 = 0.1$.

However, the relaxation time to equipartition depends on the gap between the timescales involved in the system. In our system, two timescales are involved, i.e., the timescale of the vibration of the molecule and that of the interaction between beads in the molecule and solvent particles. These timescales are determined by the spring constants k and k_α. When the difference between these timescales is larger, the relaxation to the equipartition takes a long time [18]. The relaxation time obeys the Boltzmann-Jeans law and the details are shown in Refs. [17,18]. Furthermore, the relaxation process is not monotonic; rather, the time-averaged kinetic energy of the solvent particle shows an overshoot. In fact, as the spring constant k increases, we observe that the kinetic energy of the solvent starting from zero increases gradually, and it exceeds that of the chain molecule, as shown in Fig. 4(b). After some period, it gradually relaxes to the equipartitioned value. For the potential energy of the spring in the molecule, we see that $\overline{V_{\rm mol}}(t)$ increases gradually, and it converges to half of the equipartitioned value.

As the spring constant k becomes considerably larger in addition to the longer relaxation time, a plateau appears as shown in Fig. 4(c) after $\overline{K_{\rm sol}}(t)$ exceeds $\overline{K_{\rm mol}}(t)$. Because the plateau becomes wider as k increases, the system is almost stationary. We call this stationary state in which the system settles in the plateau a QE. After a long QE, the system relaxes to the equipartition. The duration of QE becomes longer with k. Moreover, the duration increases as $\exp(\sqrt{k})$, which is consistent with the Boltzmann-Jeans conjecture, as reported in Refs. [17,18]. Hereafter, we clarify how the kinetic energies of the bead molecule and solvent particles are distributed during the QE.

During the QE, we observed that the average kinetic energy of solvent particles was larger than that of the beads in the molecule (see Fig. 4). This phenomena is a universal feature in a sense that it appears for both systems of the chain and network molecules and is irrelevant to the connection structure of the molecule. To characterize this difference in QE, we observe the kinetic energy of each particle at which the QE state persists, i.e., $\overline{K_{\rm mol}^{\rm QE}} = \overline{K_{\rm mol}}(t_{\rm QE})$ and $\overline{K_{\rm sol}^{\rm QE}} = \overline{K_{\rm sol}}(t_{\rm QE})$, where $t_{\rm QE}$ is a typical time during the QE state; we use $t_{\rm QE} = 10^4$. For QE, we find that the following inequality holds:

$$\overline{K_{\rm mol}}(t_{\rm QE}) < \overline{K_{\rm sol}}(t_{\rm QE}).$$

In the following subsections, we consider the time-averaged kinetic energy distribution for beads in the molecule and solvent particles in QE by changing the molecular size and structure and the number of solvent particles.

B. Quasiequilibrium for the chain molecule

The kinetic energies $\overline{K_{\rm chain}^{\rm QE}}$ and $\overline{K_{\rm sol}^{\rm QE}}$ that depend on the number of beads in a chain molecule are shown in Fig. 5. Both energies decrease gradually, and the difference between them converges to a constant value as N_b, i.e., the length of the chain molecule, increases. It is stressed that $\overline{K_{\rm mol}}(t_{\rm QE}) < \overline{K_{\rm sol}}(t_{\rm QE})$ holds for any chain length. Indeed, as shown in Fig. 5(b), the ratio of the kinetic energy of the chain molecule to that of the solvent converges to a value as N_b increases. The ratio is always larger than one, and it increases gradually as N_b increases. This clearly shows that the kinetic energy of the solvent is always larger than that of the chain molecules during QE.

Figure 6(a) shows the $\overline{K_{\rm chain}^{\rm QE}}$ and $\overline{K_{\rm sol}^{\rm QE}}$ dependency on the number of solvent particles N_s. Both energies gradually decrease as N_s increases. However, the ratio $\overline{K_{\rm sol}^{\rm QE}}/\overline{K_{\rm chain}^{\rm QE}}$ does not depend on the number of solvent particles, as shown in Fig. 6(b). These results support that in QE, the kinetic energy

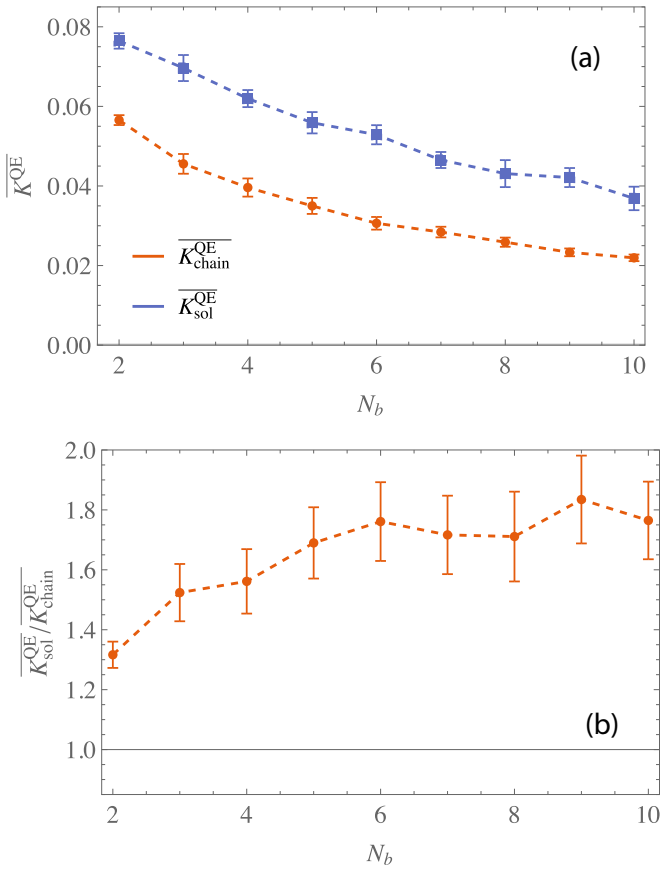

FIG. 5. (a) Time-averaged kinetic-energies of the chain molecule $\overline{K^{\rm QE}_{\rm chain}}$ and the solvent $\overline{K^{\rm QE}_{\rm sol}}$ as a function of chain length N_b. The circles and squares on the error bars are $\overline{K^{\rm QE}_{\rm chain}}$ and $\overline{K^{\rm QE}_{\rm sol}}$, respectively. (b) The ratio $\overline{K^{\rm QE}_{\rm mol}}/\overline{K^{\rm QE}_{\rm sol}}$ is shown as a function of N_b. The error bars show the 95% confidence interval, which is estimated using samples starting from different $\mathscr{M}$ initial conditions. $k = 1000$, $N_s = 2$, $k = 1000$, $\mathscr{M} = 10$, $T_{\rm QE} = 10^4$, and $E_0 = 0.3$.

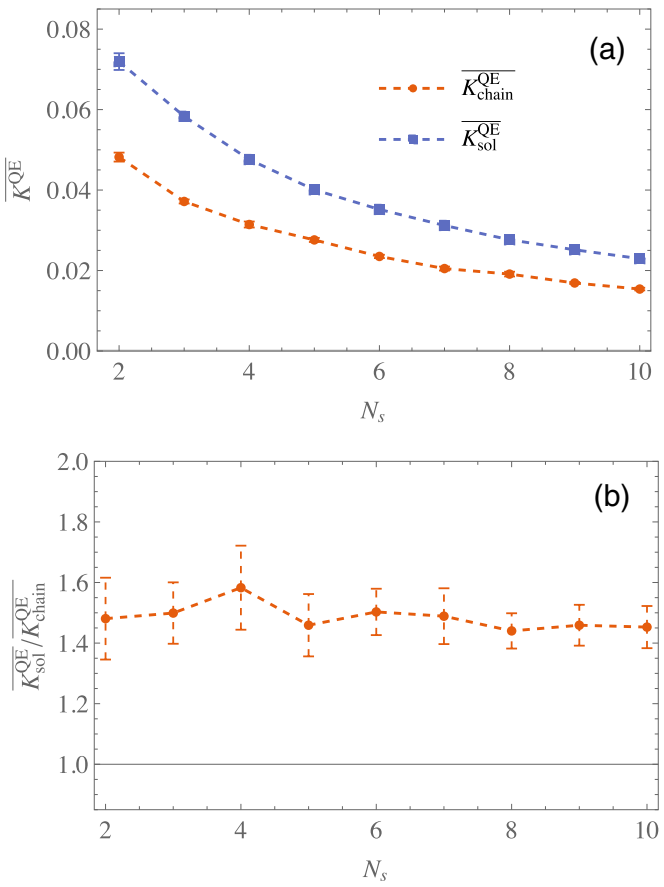

FIG. 6. (a) Time-averaged kinetic energies of the chain molecules $\overline{K^{\rm QE}_{\rm chain}}$ (circles) and the solvent particles $\overline{K^{\rm QE}_{\rm sol}}$ (squares) in QE as a function of the number of solvent particles N_s. (b) The ratio $\overline{K^{\rm QE}_{\rm sol}}/\overline{K^{\rm QE}_{\rm chain}}$ dependency on N_s. The other parameters and the error bars are the same as those in Fig. 5.

of the solvent particles is always larger than that of the chain molecule. It is stressed that the ratio is independent of the number of solvent particles, which is usually large in reality.

C. Quasiequilibrium for the network molecule

We consider the energy distribution during QE for the network molecule wherein the beads are densely connected by linear springs as shown in Fig. 2. To contrast the effect of the number of springs which plays a crucial role in energy distribution, we consider the complete graph as the connection topology for the network molecule. The Hamiltonian is defined by Eqs. (10) and (11). In Fig. 7(a), the time-averaged kinetic energy for the network molecule and that for solvent particles $\overline{K^{\rm QE}_{\rm net}}$ and $\overline{K^{\rm QE}_{\rm sol}}$ are shown as a function of N_b, i.e., the number of beads in the network molecule. While $\overline{K^{\rm QE}_{\rm net}}$ gradually decreases with N_b, $\overline{K^{\rm QE}_{\rm sol}}$ does not depend on N_b. In Fig. 7(b), the ratio $\overline{K^{\rm QE}_{\rm sol}}/\overline{K^{\rm QE}_{\rm net}}$ is shown as a function of N_b. In contrast to the chain molecule, the ratio increases linearly with N_b and is always larger than one. In Fig. 8(a), the time-averaged kinetic energy $\overline{K^{\rm QE}_{\rm net}}$ and $\overline{K^{\rm QE}_{\rm sol}}$ are shown as a function of N_s. The both time-averaged kinetic energies decrease with N_s. The ratio $\overline{K^{\rm QE}_{\rm sol}}/\overline{K^{\rm QE}_{\rm net}}$ does not depends on N_s as shown in Fig. 8(b).

In this section, we numerically show that the kinetic energy of the solvent particle is always larger than that of the bead in the molecule during QE, i.e., $\overline{K_{\rm mol}}(t_{\rm QE}) < \overline{K_{\rm sol}}(t_{\rm QE})$. This fact is independent of the molecular structure, the number of beads in the molecule, and the number of solvent particles. In other words, the solvent particles are more energetic than the beads in the molecule during the QE. The number of springs in the molecule plays a crucial role in determining the distribution of energy.

V. THEORETICAL EXPLANATION

A. Equipartition theorem

Let us recall the equipartition theorem. Usually, the theorem states that the thermal average of the kinetic energy in the equilibrium is given by

$$\langle \varepsilon \rangle_\beta \equiv \left\langle \frac{(p_i^x)^2}{2m} \right\rangle_\beta = \left\langle \frac{(p_i^y)^2}{2m} \right\rangle_\beta = \frac{1}{2\beta}, \tag{20}$$

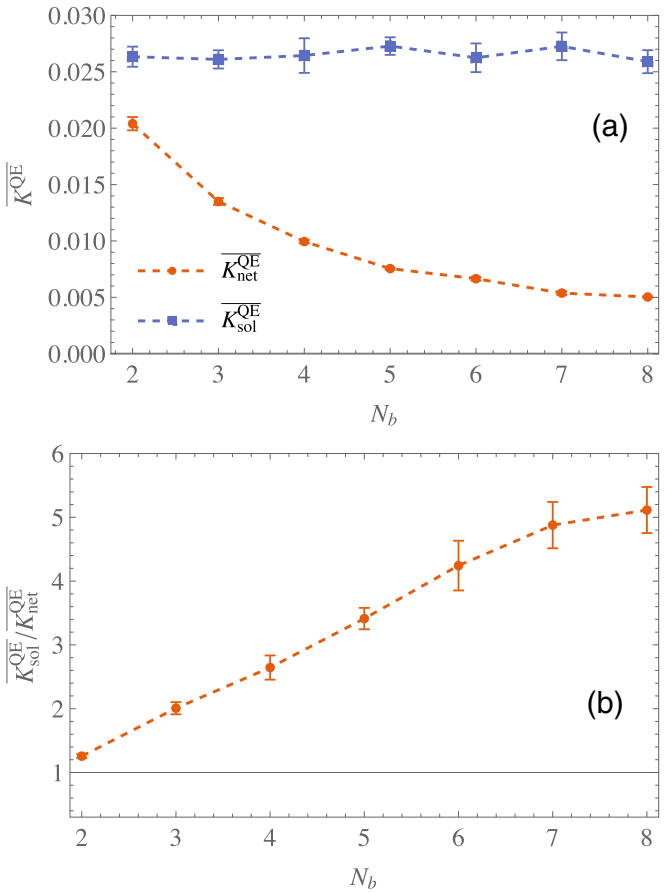

FIG. 7. (a) The time-averaged kinetic energies of the beads in the network molecules and those of the solvent particles are shown as a function of the number of beads by the circles and squares on the error bars, respectively. (b) The ratio of the kinetic energy of the solvent particle to that of the network molecule is shown as a function of the number of beads. $N_b = 6$ and $E_0 = 0.1$. The other parameters are the same as those in Fig. 5.

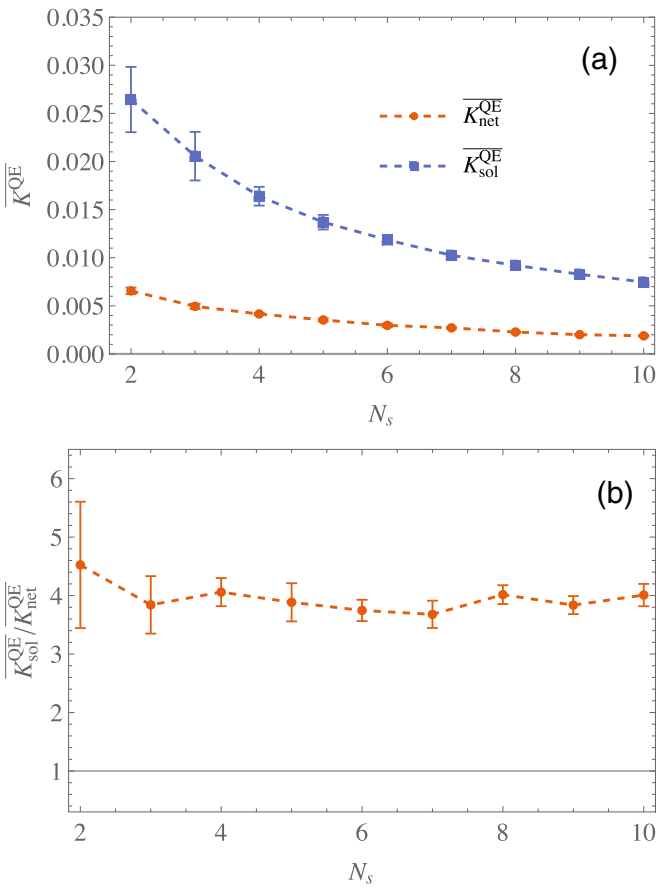

FIG. 8. (a) Time-averaged kinetic energies of the beads in the network molecules and solvent particles are shown by the circles and the squares on the error bars, respectively. (b) The ratio of the kinetic energy of the solvent to that of the network molecule is shown as a function of the number of solvent particles N_s. The ratio does not depend on N_s. The other parameters are the same as those in Fig. 7.

where p_i^x and p_i^y are the momenta of the x and y directions of particle i in the system, respectively. The symbol $\langle \cdots \rangle_\beta$ represents the thermal average at the inverse temperature $\beta \equiv 1/k_B T$ and is defined as

$$\langle f(q,p)\rangle_\beta \equiv \frac{1}{Z}\int f(q,p)e^{-\beta H(p,q)}d\Gamma \tag{21}$$

for any function of general coordinates and their conjugate momenta $f(q,p)$. Here $d\Gamma$ denotes a volume element of the phase space and Z represents a partition function. The key point of the theorem is that the kinetic energy is quadratic in the momentum. Further, if any energy is described by the harmonic form of the coordinate q, then we can show that the thermal average of such potential energy also takes the same value [21]. For example, the thermal average of the potential energy with the form $U(q) = \frac{1}{2}q^2$ is

$$\langle U(q)\rangle_\beta = \frac{1}{2\beta} = \langle \varepsilon \rangle_\beta. \tag{22}$$

Consider the following Hamiltonian, which is represented by the sum of the harmonic form:

$$\mathscr{H} = \sum_{i=1}^{f}\frac{(p_i^x)^2 + (p_i^y)^2}{2m_i} + \sum_{i=1}^{f}\frac{1}{2}k_i q_i^2,$$

where $2f$ is the number of degrees of freedom. Then the thermal average of the total energy of such a system becomes

$$\langle \mathscr{H}\rangle_\beta = \frac{\mathscr{F}_{sys}}{2\beta} = \mathscr{F}_{sys}\langle \varepsilon \rangle_\beta, \tag{23}$$

where we define $\mathscr{F}_{sys}$ as the number of independent harmonic terms that enter into the Hamiltonian. For the above Hamiltonian, the total number of harmonic degrees is $\mathscr{F}_{sys} = 3f$.

B. Theoretical estimation of averaged kinetic energies for quasiequilibrium

We now estimate the kinetic energy of beads in the molecule and solvent particles by adopting the equipartition theorem for QE. To this end, we assume the following. First, we assume that the thermal average of the total energy $\langle \mathscr{H}\rangle_\beta$ is equal to E_0. Second, anharmonic potential terms are approximated by harmonic ones. The second assumption is valid

for a scenario wherein the amplitude of the vibrational oscillation is sufficiently small because the spring coefficient is sufficiently large.

Based on these assumptions, the number of independent harmonic terms entering the Hamiltonian is denoted by $\mathscr{F}_{\rm sys}$; we refer to them as the harmonic degrees (HDs). Thus, we consider that the total energy E_0 is equally distributed into $\mathscr{F}_{\rm sys}$ HDs. Therefore, in equilibrium, the energy per HD can be estimated by

$$\langle\langle \varepsilon \rangle\rangle \equiv \frac{E_0}{\mathscr{F}_{\rm sys}}. \tag{24}$$

Hereafter, we represent $\langle\langle \cdots \rangle\rangle$ as the kinetic energy per HD by adopting the equipartition theorem to the Hamiltonian dynamical system.

To estimate the energy per HD, we divide the system into two subsystems, A and B, where subsystem A has frozen HDs and B does not have such frozen degrees. Furthermore, we denote the number of HDs in equilibrium for A and B by $\mathscr{F}_A$ and $\mathscr{F}_B$, respectively. Thus, the total number of HDs of the system is $\mathscr{F}_{\rm sys} = \mathscr{F}_A + \mathscr{F}_B$. When we adopt the equipartition in the equilibrium, the equally distributed energy per HD can be estimated by

$$\langle\langle \varepsilon \rangle\rangle = \langle\langle \varepsilon^A \rangle\rangle = \langle\langle \varepsilon^B \rangle\rangle = \frac{E_0}{\mathscr{F}_{\rm sys}} = \frac{E_0}{\mathscr{F}_A + \mathscr{F}_B}. \tag{25}$$

A schematic of the energy distribution in the equilibrium is shown in the top panel of Fig. 9. In the case of QE, the time-averaged spring energy is almost zero if the spring coefficient is sufficiently large, as shown in Fig. 4(c). This means that the vibrational motion of the molecule is frozen in the sense that there are no energy exchanges between them and the other degrees. To estimate the energy per HD in QE, we describe the number of HDs of subsystem A as the sum of the number of kinetic HDs and that of the potential HDs, i.e., $\mathscr{F}_A = \mathscr{F}_{K_A} + \mathscr{F}_{V_A}$, where $\mathscr{F}_{K_A}$ denotes the number of HDs for the kinetic part, and $\mathscr{F}_{V_A}$ denotes the number of HDs for the potential part entered in the Hamiltonian of subsystem A. When the number of stiff springs in A is $\mathscr{F}_Z$, the number of active HDs in QE is $\mathscr{F}_A^{\rm QE} = \mathscr{F}_A - 2\mathscr{F}_Z$. Here the factor 2 originates from the fact that these stiff springs behave as rigid links, and they act as constraints for molecular motion. Thus, the number of HDs for the kinetic part is reduced to $\mathscr{F}_{K_A} - \mathscr{F}_Z$, and that of the HDs for the potential part is reduced to $\mathscr{F}_{V_A} - \mathscr{F}_Z$. The bead-spring system in QE behaves as a system with constraints in equilibrium [17,18], and the generalized equipartition theorem holds for such constrained systems [21]. Therefore, we adopt the equipartition theorem by simply replacing the active HDs. We derive the energy per HD in QE as

$$\langle\langle \varepsilon \rangle\rangle_{\rm QE} = \frac{E_0}{\mathscr{F}_{\rm sys}^{\rm QE}} = \frac{E_0}{\mathscr{F}_A - 2\mathscr{F}_Z + \mathscr{F}_B}. \tag{26}$$

Then the total energies attributed to subsystems A and B are

$$\langle\langle E^A \rangle\rangle_{\rm QE} = \mathscr{F}_A^{\rm QE} \langle\langle \varepsilon \rangle\rangle_{\rm QE}, \tag{27}$$

$$\langle\langle E^B \rangle\rangle_{\rm QE} = \mathscr{F}_B^{\rm QE} \langle\langle \varepsilon \rangle\rangle_{\rm QE}, \tag{28}$$

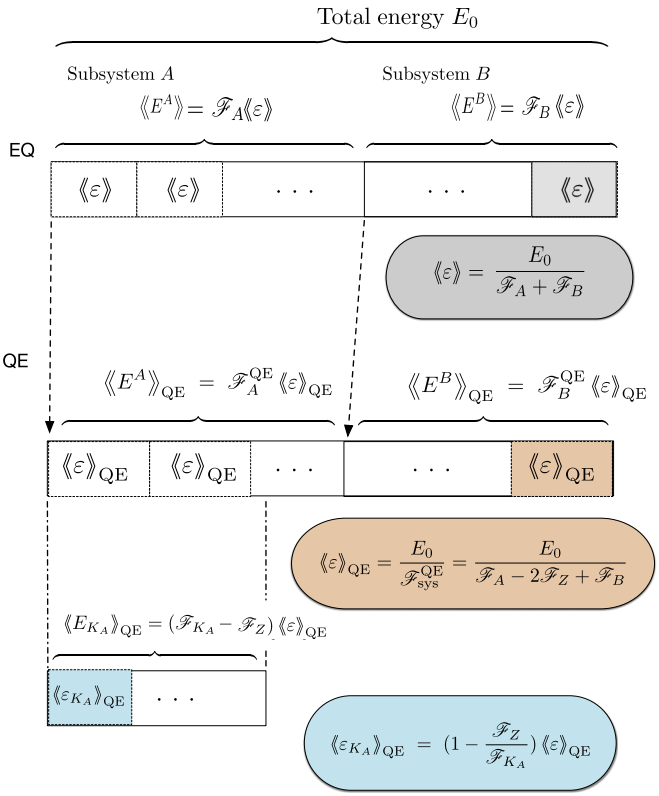

FIG. 9. Schematic for the energy distribution per HD based on the equipartition theorem. The top panel shows the equipartition state in equilibrium, where the total energy E_0 is equally distributed to the total number of HDs, $\mathscr{F}_{\rm sys} = \mathscr{F}_A + \mathscr{F}_B$. The middle panel shows the QE state at which the total energy is equally distributed to "active" HDs, i.e., $\mathscr{F}_{\rm sys}^{\rm QE} = \mathscr{F}_A - 2\mathscr{F}_Z + \mathscr{F}_B$. The bottom panel shows that the kinetic energy of subsystem A is redistributed according to the number of kinetic HDs, that is, $\mathscr{F}_{K_A}$.

respectively, where $\mathscr{F}_A^{\rm QE} = \mathscr{F}_A - 2\mathscr{F}_Z$ and $\mathscr{F}_B^{\rm QE} = \mathscr{F}_B$. A schematic of the energy distribution in QE is shown in the middle panel of Fig. 9. The total kinetic energy of subsystem A becomes $\langle\langle E_{K_A} \rangle\rangle_{\rm QE} = (\mathscr{F}_{K_A} - \mathscr{F}_Z)\langle\langle \varepsilon \rangle\rangle_{\rm QE}$. Because we observe kinetic energy per bead, we divide the total kinetic energy by the number of kinetic HDs. Therefore, the kinetic energies per bead and particle for subsystems A and B are

$$\langle\langle \varepsilon_{K_A} \rangle\rangle_{\rm QE} = \frac{\mathscr{F}_{K_A} - \mathscr{F}_Z}{\mathscr{F}_{K_A}} \langle\langle \varepsilon \rangle\rangle_{\rm QE}, \tag{29}$$

$$\langle\langle \varepsilon_{K_B} \rangle\rangle_{\rm QE} = \frac{\mathscr{F}_{K_B}^{\rm QE}}{\mathscr{F}_{K_B}} \langle\langle \varepsilon \rangle\rangle_{\rm QE} = \langle\langle \varepsilon \rangle\rangle_{\rm QE}, \tag{30}$$

respectively. Because subsystem B does not have frozen degrees, the number of HDs in the kinetic parts in QE is the same as that in equilibrium, i.e., $\mathscr{F}_{K_B} = \mathscr{F}_{K_B}^{\rm QE}$, and $\mathscr{F}_Z < \mathscr{F}_{K_A}$,

$$\langle\langle \varepsilon_{K_A} \rangle\rangle_{\rm QE} = \left(1 - \frac{\mathscr{F}_Z}{\mathscr{F}_{K_A}}\right) \langle\langle \varepsilon \rangle\rangle_{\rm QE}, \tag{31}$$

$$< \langle\langle \varepsilon \rangle\rangle_{\rm QE} = \langle\langle \varepsilon_{K_B} \rangle\rangle_{\rm QE}. \tag{32}$$

Therefore, the distributed energy per HD for subsystem A with a frozen degree is always smaller than that without the

frozen degrees. A schematic is shown in the bottom panel of Fig. 9. Further, we obtain the ratio as

$$\frac{\langle\langle \varepsilon_{K_A}\rangle\rangle_{\rm QE}}{\langle\langle \varepsilon_{K_B}\rangle\rangle_{\rm QE}} = 1 - \frac{\mathscr{F}_Z}{\mathscr{F}_{K_A}}. \tag{33}$$

This means that the ratio does not depend on the number of HDs for subsystem B. For bead-spring systems, since B corresponds to the solvent, we conclude that the kinetic energy of each solvent particle is always larger than that of the beads in the molecule during QE. We adopt these results for the chain and network molecules in the solvent, and verify the numerical results.

C. Averaged kinetic energy for chain molecule in quasiequilibrium

We apply the above theory to the chain molecule. In the case of the chain molecule in the solvent, the system can be divided into a chain molecule corresponding to subsystem A and the solvent particles corresponding to subsystem B. The number of HDs for chain molecule in the equilibrium is

$$\mathscr{F}_{\rm chain} = 2N_b + (N_b - 1), \tag{34}$$

where N_b and N_s are the number of beads in the molecule and in the solvent, respectively. The first term corresponds to the number of HDs for the kinetic part of the beads in the molecule, and the second term corresponds to the number of HDs for the potential part of the molecule. The effective number of HDs for the solvent is

$$\mathscr{F}_{\rm sol} = 2N_s + \gamma N_s, \tag{35}$$

where the first and second terms correspond to the kinetic and potential parts of the solvent, respectively. Because the interaction between the solvent and molecule has a cut-off distance ℓ_α, as in Eq. (5), it cannot be treated by the potential energy as a harmonic form. Thus, we estimate the interaction energy as a linear function of the number of solvent particles with coefficient γ. The parameter γ represents the effective quadratic degrees of freedom for the interaction energy between beads and solvent particles. Here, we used cut-off distance for the interaction, and thus it is not a quadratic form. Setting γ to zero corresponds to neglecting the interactions between beads and solvent particles; if $\gamma = 1$, then we treat the interaction as quadratic potential. Here we select the value $\gamma = 1/4 \in [0, 1]$ by fitting the numerical data.

Therefore, using Eq. (34) and (35), the energy per HD in the equilibrium is given by

$$\langle\langle \varepsilon\rangle\rangle = \frac{E_0}{\mathscr{F}_{\rm sys}} = \frac{E_0}{3N_b - 1 + (2+\gamma)N_s}, \tag{36}$$

where $\mathscr{F}_{\rm sys} = \mathscr{F}_{\rm chain} + \mathscr{F}_{\rm sol}$ is the effective number of estimated HDs for the system. In QE, the energy exchange between the vibration of the molecule and the other part is prevented. The number of stiff springs is $\mathscr{F}_Z = N_b - 1$, and thus the number of degrees of motion of the chain molecule is reduced to $\mathscr{F}^{\rm QE}_{K_{\rm chain}} = 2N_b - (N_b - 1)$ because the distance between the beads in a molecule is almost constant in QE. In other words, each spring acts as a rigid link, and the molecule behaves as if the motion has $N_b - 1$ constraints. Thus, the total number of frozen HDs is $2\mathscr{F}_Z = 2(N_b - 1)$ and $\mathscr{F}^{\rm QE}_{\rm sys} = \mathscr{F}_{\rm chain} - 2\mathscr{F}_Z + \mathscr{F}_{\rm sol}$. The energy distributed to these HDs is

$$\langle\langle \varepsilon\rangle\rangle_{\rm QE} = \frac{E_0}{\mathscr{F}^{\rm QE}_{\rm sys}} = \frac{E_0}{N_b + 1 + (2+\gamma)N_s}. \tag{37}$$

Therefore, the kinetic energies for chain beads and solvent particles can be estimated as

$$\langle\langle \varepsilon_{\rm chain}\rangle\rangle_{\rm QE} = \frac{E_0}{N_b + 1 + (2+\gamma)N_s}\left(\frac{N_b+1}{3N_b-1}\right), \tag{38}$$

$$\langle\langle \varepsilon_{\rm sol}\rangle\rangle_{\rm QE} = \frac{E_0}{N_b + 1 + (2+\gamma)N_s}, \tag{39}$$

and the quasiequilibrium to equilibrium ratios for these kinetic energies are

$$\frac{\langle\langle \varepsilon_{\rm chain}\rangle\rangle_{\rm QE}}{\langle\langle \varepsilon\rangle\rangle} = \frac{N_b - 1}{2N_b}\langle\langle \varepsilon\rangle\rangle_{\rm QE} = \left(\frac{\langle\langle \varepsilon_{\rm sol}\rangle\rangle_{\rm QE}}{\langle\langle \varepsilon\rangle\rangle}\right)\left(\frac{1}{2} + \frac{1}{2N_b}\right), \tag{40}$$

$$\frac{\langle\langle \varepsilon_{\rm sol}\rangle\rangle_{\rm QE}}{\langle\langle \varepsilon\rangle\rangle} = 1 + \frac{2(1-N_b)}{N_b + 1 + (2+\gamma)N_s}. \tag{41}$$

Comparisons between these analytic expressions and numerical experiments are shown in Fig. 10. In these figures, the theoretical expressions are indicated by the dashed and dotted-dashed lines. The dashed lines correspond to the theoretical estimations using Eq. (40) with $\gamma = 1/4$, and the dotted-dashed lines correspond to the theoretical estimation using Eq. (41) with $\gamma = 1/4$.

The time-averaged kinetic energy in the QE dependency on the number of beads N_b and solvent particles N_s is in good agreement with the theoretical estimations. The ratio $\langle\langle \varepsilon_{\rm sol}\rangle\rangle_{\rm QE}/\langle\langle \varepsilon_{\rm chain}\rangle\rangle_{\rm QE}$ does not depend on the number of solvent particles and the parameter γ, that is,

$$\frac{\langle\langle \varepsilon_{\rm sol}\rangle\rangle_{\rm QE}}{\langle\langle \varepsilon_{\rm chain}\rangle\rangle_{\rm QE}} = 2 - \frac{2}{N_b + 1}. \tag{42}$$

This means that the kinetic energy of the solvent particle is twice that of the long chain molecule for any number of solvent particles, and for a long chain molecule with any fixed N_s, we get

$$\lim_{N_b\to\infty} \frac{\langle\langle \varepsilon_{\rm chain}\rangle\rangle_{\rm QE}}{\langle\langle \varepsilon\rangle\rangle} = \frac{3}{2}.$$

$$\lim_{N_b\to\infty} \frac{\langle\langle \varepsilon_{\rm sol}\rangle\rangle_{\rm QE}}{\langle\langle \varepsilon\rangle\rangle} = 3.$$

The kinetic energy per HD for both the chain bead and solvent particles in QE is always higher than that for the equilibrium values. For a large number of solvent particles with fixed N_b, we derive that

$$\lim_{N_s\to\infty} \frac{\langle\langle \varepsilon_{\rm chain}\rangle\rangle_{\rm QE}}{\langle\langle \varepsilon\rangle\rangle} = \frac{2}{3}.$$

$$\lim_{N_s\to\infty} \frac{\langle\langle \varepsilon_{\rm sol}\rangle\rangle_{\rm QE}}{\langle\langle \varepsilon\rangle\rangle} = 1.$$

The kinetic energy of the solvent particles in QE converges to the equilibrium value as N_s increases, while the kinetic energy of the chain bead in QE is always lower than that of the equilibrium value.

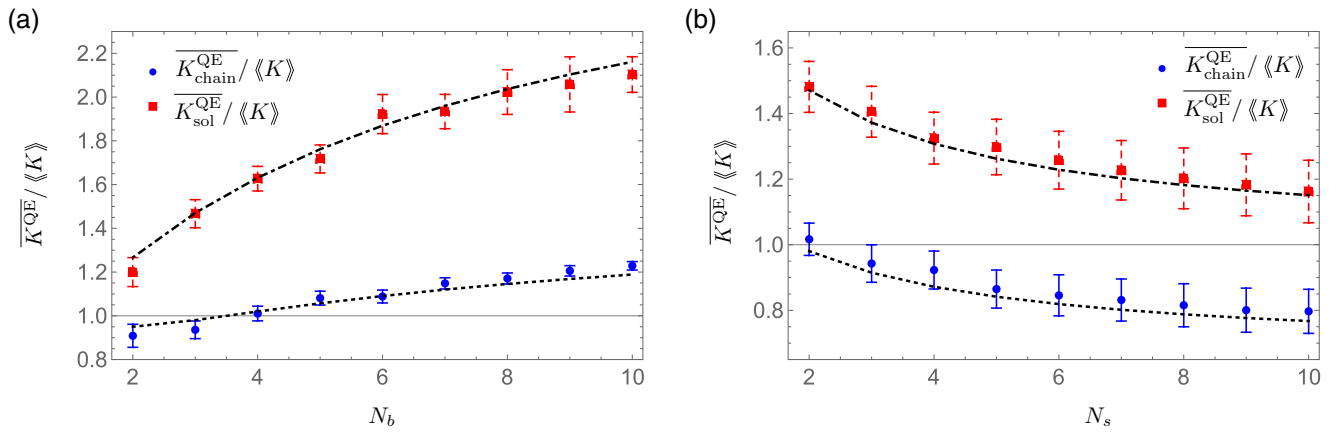

FIG. 10. (a) Time-averaged kinetic energies for beads in chain molecules and solvent particles normalized by their equilibrium values as a function of N_b are shown by circles and squares on the error bars, respectively. The dashed and the dotted-dashed lines are the theoretical estimations obtained using Eqs. (40) and (41) with $N_s = 2$ and $\gamma = 1/4$, respectively. (b) Time-averaged kinetic energies for beads and solvent particles normalized by their equilibrium values are shown as a function of the number of solvent particles N_s. The dashed and the dotted-dashed lines are the same as in (a) with $N_b = 3$. $k = 1000$ and $\mathscr{M} = 10$, and the other parameters are the same as those in Fig. 6.

D. Averaged kinetic energy for network molecule in quasiequilibrium

We consider the theoretical estimation of the kinetic energy per HD for the network molecule. Here we consider the complete graph as a connection topology for the molecule; the number of springs in the molecule is ${}_{N_b}C_2 = N_b(N_b-1)/2$. Thus, the number of springs is larger than that of the beads when N_b is larger than three. When these springs are stiff, the motion of the network molecule is restricted by the many springs, and it behaves as one particle. Therefore, only the translational and rotational degrees of freedom remain in QE; thus, $\mathscr{F}_{\rm net}^{\rm QE} = 3$. The number of independent HDs for the potential energy of the springs in the molecule can be considered in the following manner. Let us consider a simple scenario wherein the two beads are connected by two different springs with spring constants k_1 and k_2. In this case, the two springs are not independent; rather, they behave as one spring with a spring constant $k_1 + k_2$. Thus, the number of independent HDs for such a molecule is five, to which the energy is equally distributed, i.e., four kinetic HDs and one potential HD for these springs. In the case of a molecule comprising four beads, any pair of beads is connected by a stiff spring. The connection topology is a complete graph, and there are six springs in the molecule. The motion of these springs is no longer independent, and there are four independent springs in this case. For the molecule with a complete-graph connection topology, there are $N_b(N_b-1)/2$ springs; however, the number of independent HDs entered in such a potential energy is

$$\mathscr{F}_{\rm spring} = 2N_b - 3. \tag{43}$$

The number of independent springs is the same as the degree of the framework, which is the rank of the rigid matrix in the literature [22–25]. In Appendix, we check the number of independent HDs for network molecules by directly calculating the thermal average of the potential energy using the Markov-chain Monte Carlo (MCMC) method.

This estimation of the number of independent HDs can be explained intuitively as follows. When the spring constant is sufficiently large, we observe that springs act as constraints for the motion of the beads in the molecule, and the molecule behaves as one particle, as explained previously. In fact, during QE, the energy exchange between the springs and other parts is prevented; thus, the potential energy for springs is almost zero, which is the initial value. Then, the total number of degrees for the network molecule is the sum of the transnational and rotational degrees. Thus, the following equation holds:

$$\mathscr{F}_{\rm net}^{\rm QE} = 2N_b - \mathscr{F}_Z = 3, \tag{44}$$

where $\mathscr{F}_Z = \mathscr{F}_{\rm spring}$. The effective number of HDs in the solvent part is the same as in the case of the chain molecule, as explained in the previous subsection:

$$\mathscr{F}_{\rm sol} = 2N_s + \gamma N_s.$$

Therefore, the effective number of HDs for the whole system can be estimated using

$$\begin{aligned}\mathscr{F}_{\rm sys} &= 2N_b + \mathscr{F}_{\rm spring} + \mathscr{F}_{\rm sol}\\ &= 4N_b - 3 + (2+\gamma)N_s,\end{aligned} \tag{45}$$

$$\begin{aligned}\mathscr{F}_{\rm sys}^{\rm QE} &= 2N_b - \mathscr{F}_Z + \mathscr{F}_{\rm sol}\\ &= 3 + (2+\gamma)N_s.\end{aligned} \tag{46}$$

Thus, the distributed energy per HD during QE is given as

$$\langle\langle\varepsilon\rangle\rangle_{\rm QE} = \frac{E_0}{\mathscr{F}_{\rm sys}^{\rm QE}} = \frac{E_0}{3+(2+\gamma)N_s}. \tag{47}$$

Using the above estimation of the number of HDs and assuming that the total energy is distributed equally to these degrees, we obtain the average energy per HD as

$$\langle\langle\varepsilon_{\rm net}\rangle\rangle_{\rm QE} = \langle\langle\varepsilon\rangle\rangle_{\rm QE}\frac{\mathscr{F}_{\rm net}^{\rm QE}}{\mathscr{F}_{\rm net}} = \frac{3E_0}{\{3+(2+\gamma)N_s\}(4N_b-3)}, \tag{48}$$

$$\langle\langle\varepsilon_{\rm sol}\rangle\rangle_{\rm QE} = \langle\langle\varepsilon\rangle\rangle_{\rm QE} = \frac{E_0}{3+(2+\gamma)N_s}, \tag{49}$$

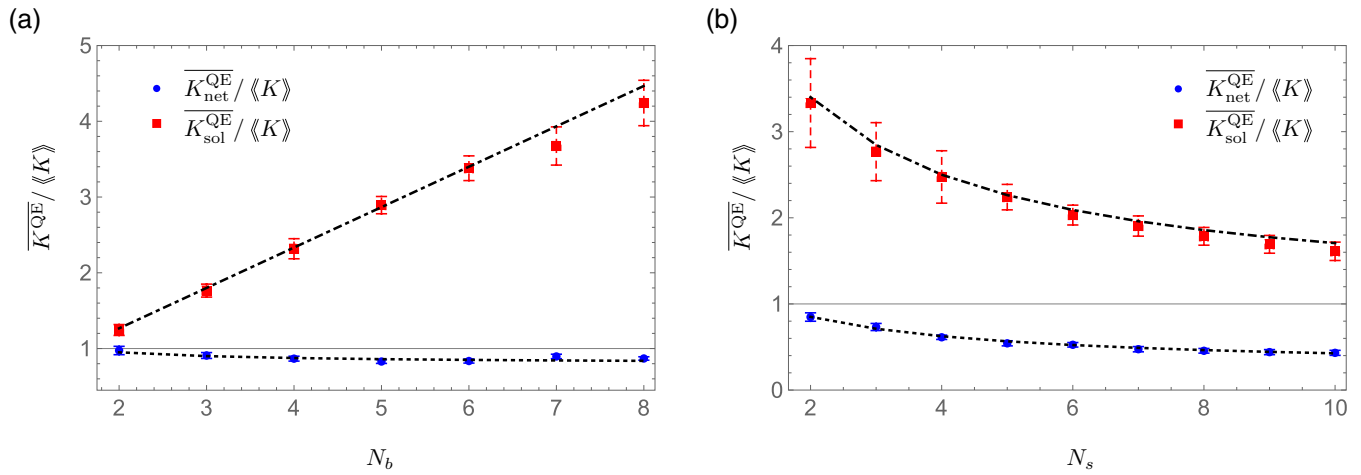

FIG. 11. (a) Time-averaged kinetic energies for beads in network molecules and solvent particles normalized by their equilibrium values as a function of the number of beads N_b are shown by circles and squares on the error bars, respectively. The dashed and the dotted-dashed lines represent the theoretical estimations using Eqs. (50) and (51) with $N_s = 2$. (b) The same as in (a) with the function of the number of solvent particles N_s. The dashed and dotted-dashed lines are the same as in (a) with $N_b = 6$. $E_0 = 0.1$. The other parameters are the same as those in Fig. 6.

and the ratios to its equilibrium value $\langle\langle\varepsilon\rangle\rangle = E_0/\mathscr{F}_{\rm sys}$ are

$$\frac{\langle\langle\varepsilon_{\rm net}\rangle\rangle_{\rm QE}}{\langle\langle\varepsilon\rangle\rangle} = \left\{1 + \frac{4N_b - 6}{3 + (2+\gamma)N_s}\right\}\frac{3}{2N_b}, \tag{50}$$

$$\frac{\langle\langle\varepsilon_{\rm sol}\rangle\rangle_{\rm QE}}{\langle\langle\varepsilon\rangle\rangle} = \left\{1 + \frac{4N_b - 6}{3 + (2+\gamma)N_s}\right\}. \tag{51}$$

The time-averaged energy dependency on the number of beads N_b and solvent particles N_s are plotted with these theoretical estimations, as shown in Figs. 11(a) and 11(b), respectively. The dashed and dotted-dashed lines in these figures represent the theoretical estimations by Eqs. (50) and (51) with $\gamma = 1/4$, respectively. These theoretical estimations are in good agreement with the numerical results.

In the case of the network molecule, the ratio of these averaged energies is inversely proportional to N_b as

$$\frac{\langle\langle\varepsilon_{\rm net}\rangle\rangle_{\rm QE}}{\langle\langle\varepsilon_{\rm sol}\rangle\rangle_{\rm QE}} = \frac{3}{2N_b}, \tag{52}$$

and does not depend on the parameter γ. This implies that for a molecule composed of a large number of atoms (e.g., a biomolecule), the averaged kinetic energy of such a molecule becomes considerably lower than that of a solvent particle during QE.

For a large number of solvent particles with a fixed number of beads, we get

$$\lim_{N_s\to\infty}\frac{\langle\langle\varepsilon_{\rm net}\rangle\rangle_{\rm QE}}{\langle\langle\varepsilon\rangle\rangle} = \frac{3}{2N_b}.$$

$$\lim_{N_s\to\infty}\frac{\langle\langle\varepsilon_{\rm sol}\rangle\rangle_{\rm QE}}{\langle\langle\varepsilon\rangle\rangle} = 1.$$

These ratios also do not depend on the parameter γ.

VI. SUMMARY

We investigated the emergence of the QE over the course of relaxation to equipartition for Hamiltonian dynamics with fast and slow timescales. We used the bead-spring model as a simple model of molecules and analyzed the energy distribution of molecules and solvents during the QE state. The model molecule is composed of the masses (beads) connected by linear springs in a two-dimensional space, which interact with solvent particles. Further, we considered the initial condition that a molecule has only translational kinetic energy without fast vibration, which means that the potential energy of the springs between the beads in the molecule is initially set to zero. For such initial conditions, the numerical simulations showed that all kinetic energies for beads in the molecule and solvent particles become equal on average, meaning that they relax to equipartition. However, the relaxation time to equipartition depends on the stiffness of the spring between the beads, which determines the timescale of the molecular vibration. The relaxation time can be extremely long when the timescale of the molecular vibration is shorter than that of the collision between the molecule and solvent particles. The relaxation time obeys the Boltzmann-Jeans law [18]. During such a long transition to equipartition, we observed that the time-averaged kinetic energy for beads and solvent particles was almost constant for a long time. We call this state the QE.

During the QE, we observed that the time-averaged kinetic energy of a solvent particle is always larger than that of the bead irrespective of the type of molecular structure (we considered two types of molecules: chain and network). In other words, the solvent particles behave more energetically than the beads in the molecule during the QE. We numerically show the time-averaged kinetic energy dependency on the number of beads and solvent particles. For chain molecules, both the molecular and solvent kinetic energies decrease as the length of the chain molecule increases. However, a network molecule, the solvent kinetic energy takes a constant value as the number of beads in the molecule increases. The ratio of molecule energy to solvent energy increases with an increase in the number of beads for both types of molecules. We state that the ratio does not depend on the number of solvent particles, which is usually large in reality. The functional forms of these dependencies are different, and the dependency is

determined by the connection topology of the molecule. To clarify these dependencies, we adopt the equipartition theorem for QE by considering "frozen degrees."

In equilibrium, the equipartition theorem states that the thermal average of the energy for all HDs is equal. Here the number of HDs denotes the number of independent harmonic terms that enter the Hamiltonian of the system. We explained that the numerical results observed in QE can be understood by adopting the equipartition theory and by estimating the effective number of HDs. The theoretical analysis is in good agreement with the numerical results.

In the case of a chain molecule, the molecular vibration is frozen, and the motion of the molecule behaves as if the distance between the beads is constant. Then the number of frozen HDs is $2(N_b - 1)$, where N_b denotes the number of beads in the chain molecule. We showed that the kinetic energy of the chain molecule in QE is lower than that in equilibrium for the short-length molecule $N_b \leqslant 3$; further, it becomes higher when $N_b > 3$. For the long chain, the energy of solvent is double that of the molecule in QE. The solvent's kinetic energy in QE is triple that in equilibrium. These results show that solvent behaves in a more energetic manner than molecule with frozen degrees.

In the case of network molecules, we determined that the energy ratio increases linearly with the number of beads in the molecule by estimating the number of "independent" springs in the molecule. This implies that large molecules with complex connection topology, such as biomolecules, are less energetic than solvents. When the number of solvent particles is larger, the kinetic energy per HD of the molecule in QE equals that of the equilibrium value. The energy of the molecule depends linearly on the inverse of the number of beads in the molecule. Both facts suggest that the energy ratio in QE does not depend on the number of solvent particles, which is usually large in reality. This suggests that QE can be observed by measuring the kinetic energy ratio, and it indicates the value of "frozen degrees" that exist in the system in QE.

The proper functioning of biomolecules occurs out of equilibrium. Recent NMR studies showed that the high mobility of terminal residues appears to change only via an amino acid [26]. The change in the amino acid causes a helical conformation, and the hydrogen bonds are regarded as "frozen degrees." Thus, introducing the "frozen degrees" may induce differences in the mobility [26]. Because QE lasts a long time, we can observe the difference in the average kinetic energy in the experiments, and through the kinetic energy ratio of the molecule to solvent, we can estimate how many frozen or resting degrees of freedom exist in the molecule. Such an inhomogeneity of energy distribution emerging from the frozen degree may be an indicator of how far it is from equilibrium, and it can shed some light on the functioning of the biomolecule.

ACKNOWLEDGMENTS

The authors thank Prof. M. Toda and Dr. Y. Y. Yamaguchi for fruitful discussions. This work was supported by Japan Society for the Promotion of Science (JSPS) KAKENHI Grants No. 24540417. T.K. thanks Chubu University for their financial support.

APPENDIX: ESTIMATION OF THE HARMONIC DEGREES USING THE MARKOV-CHAIN MONTE CARLO

In Secs. V C and V D, we adopt the equipartition theorem to estimate the energy distribution during the QE state. We use the HDs in which the energy is distributed equally to such degrees in QE. In the case of a chain molecule, the number of frozen motions originates from that of the springs in the molecule. However, for the bead-spring network molecule, if the number of springs exceeds $2N_b - 3$, then the polygon can be triangulated. This means that we cannot change the spring length independently, i.e., a change in the length of the spring leads to a change(s) in the other length(s). Thus, the potential energy of all springs is not a simple sum of the harmonic terms of the springs for such network molecules. In Sec. V D, we estimated the number of independent HDs as $\mathscr{F}_{\text{spring}} = 2N_b - 3$ for network molecules with the complete-graph connection topology. This is the same as the degree of a framework, which is the rank of a rigid matrix in the literature [22–25].

In this Appendix, we verify the number of the independent HDs for randomly connected network molecules using MCMC in equilibrium. The randomly connected network molecules with a fixed number of springs are simply generated in the following manner. The beads are located at an angle of the equilateral polygon placed on the unit circle, and the randomly selected N_{spring} pairs of beads are connected by a spring; duplicate pairs are forbidden. That is, the spring coefficient is $k_{i,j} = k$ in Eq. (11) if the i and j beads are connected; otherwise, $k_{i,j} = 0$.

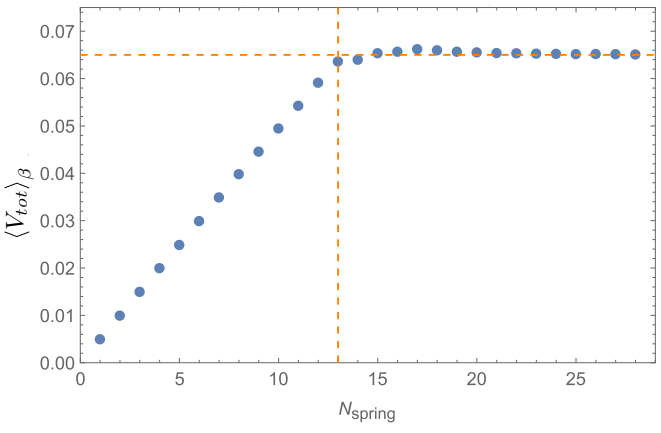

FIG. 12. Thermal-average of the total potential energy of springs for randomly connected network molecules as a function of the number of springs. The thermal average is calculated by MCMC. The vertical dashed line represents the triangulation threshold above which the total potential energy is not a sum of independent HDs. The horizontal dashed line indicates the maximum total potential energy, i.e., $\frac{2N_b-3}{2\beta}$. The parameters are $N_b = 8$, $\beta = 1$, and $\mathscr{M} = 500$.

The thermal average of the total spring energy $\langle V_{\rm tot}\rangle_\beta$ for a randomly connected network molecule with a fixed $N_{\rm spring}$ is

$$\langle V_{\rm tot}\rangle_\beta = \left\langle \sum_{i=1}^{N_b-1} \sum_{j=i+1}^{N_b} \frac{k_{i,j}}{2} (|\overrightarrow{r_j} - \overrightarrow{r_i}| - \ell_{i,j})^2 \right\rangle_\beta \tag{A1}$$

calculated by MCMC [27,28]. Further, we average the total spring energy over M different random networks. Figure 12 shows the thermal average of the total potential energy as a function of the number of springs with $N_b = 8$. The thermal average $\langle V_{\rm tot}\rangle_\beta$ increases linearly with the number of springs, whereas the number is below the regularization threshold. Above the threshold, the total potential energy takes a constant value, i.e., $\frac{2N_b-3}{2\beta}$. Therefore, the number of independent HDs for which the energy is equally distributed does not increase as the number of springs increases. The MCMC result is consistent with the previous estimation that the number of independent HDs is $2N_b - 3$ for the complete graph.

[1] E. Fermi, J. Pasta, and S. Ulam, Studies of non linear problems, Los-Alamos internal report, Document LA-1940, 1955, in *Enrico Fermi Collected Papers*, Vol. II (The University of Chicago Press, and Accademia Nazionale dei Lincei, Chicago and Roma, 1965), pp. 977–988.

[2] R. Livi, M. Pettini, S. Ruffo, M. Sparpaglione, and A. Vulpiani, Phys. Rev. A **31**, 1039 (1985).

[3] H. J. Matsuyama and T. Konishi, Phys. Rev. E **92**, 022917 (2015).

[4] L. Boltzmann, Nature (Lond.) **51**, 413 (1895).

[5] J. H. Jeans, Philos. Mag. **6**, 279 (1903).

[6] J. H. Jeans, Philos. Mag. **10**, 91 (1905).

[7] G. Benettin, A. Carati, and P. Sempio, J. Stat. Phys. **73**, 175 (1993).

[8] O. Baldan and G. Benettin, J. Stat. Phys. **62**, 201 (1991).

[9] G. Benettin, L. Galgani, and A. Giorgilli, Comm. Math. Phys. **121**, 557 (1989).

[10] G. Benettin, Prog. Theor. Phys. Suppl. **116**, 207 (1994).

[11] G. Benettin and F. Fassò, Nonlinearity **9**, 137 (1996).

[12] T. Tsuchiya, T. Konishi, and N. Gouda, Phys. Rev. E **50**, 2607 (1994).

[13] T. Tsuchiya, N. Gouda, and T. Konishi, Phys. Rev. E **53**, 2210 (1996).

[14] T. Tsuchiya, N. Gouda, and T. Konishi, Astrophys. Space Sci. **257**, 319 (1997).

[15] S. Buchenberg, D. M. Leitner, and G. Stock, J. Phys. Chem. Lett. **7**, 25 (2016).

[16] M. Doi and S. Edwards, *The Theory of Polymer Dynamics* (Clarendon Press, Oxford, 1988).

[17] T. Konishi and T. Yanagita, J. Stat. Mech. (2010) P09001.

[18] T. Konishi and T. Yanagita, J. Stat. Mech. (2016) 033201.

[19] N. Chernov and R. Markarian, *Chaotic Billiards* (American Mathematical Society, Providence, RI, 2006).

[20] B. Leimkuhler and S. Reich, *Simulating Hamiltonian Dynamics* (Cambridge University Press, Cambridge, UK, 2004).

[21] R. Kubo, H. Ichimura, T. Usui, and N. Hashitsume, *Statistical Mechanics* (North Holland, Amsterdam, 1990).

[22] J. Clerk Maxwell F.R.S., Lond., Edinb., and Dubl. Philos. Mag. J. Sci. **27**, 294 (1864).

[23] G. Laman, J. Eng. Math. **4**, 331 (1970).

[24] L. Asimow and B. Roth, Trans. Am. Math. Soc. **245**, 279 (1978).

[25] J. Graver, B. Servatius, and H. Servatius, *Combinatorial Rigidity* (American Mathematical Society, Providence, RI, 1993).

[26] Y. Miura, Eur. Biophys. J. **49**, 113 (2020).

[27] M. E. J. Newman and G. T. Barkema, *Monte Carlo Methods in Statistical Physics* (Oxford University Press, Oxford, 1999).

[28] D. Landau and K. Binder, *A Guide to Monte Carlo Simulations in Statistical Physics* (Cambridge University Press, Cambridge, UK, 2005).